iScience

CellPress
OPEN ACCESS

Article

Aedes aegypti saliva modulates inflammasome activation and facilitates flavivirus infection *in vitro*

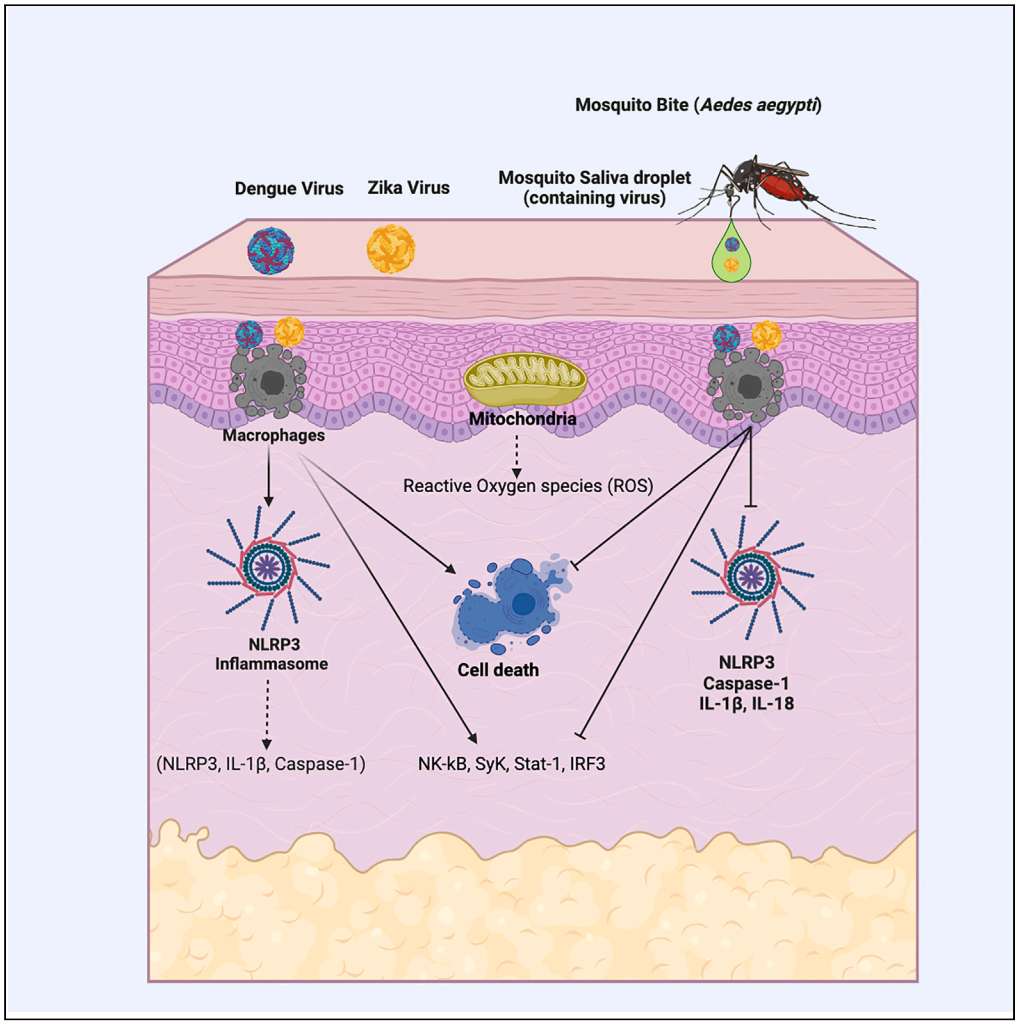

Gaurav Shrivastava, Paola Carolina Valenzuela-Leon, Karina Botello, Eric Calvo

ecalvo@niaid.nih.gov

Highlights

Mosquito saliva inhibits robust inflammasome activation during DENV and ZIKV infection

Mosquito saliva reduces mitochondrial ROS levels, impacting inflammasome

SGE reduces cell death caused by DENV and ZIKV without affecting virus replication

Mosquito saliva may dampen early virus detection via immune gene regulation

Shrivastava et al., iScience *27*, 108620
January 19, 2024
https://doi.org/10.1016/j.isci.2023.108620

iScience

CellPress
OPEN ACCESS

Article

Aedes aegypti saliva modulates inflammasome activation and facilitates flavivirus infection *in vitro*

Gaurav Shrivastava,[1] Paola Carolina Valenzuela-Leon,[1] Karina Botello,[1] and Eric Calvo[1,2,*]

SUMMARY

Mosquito borne flaviviruses such as dengue and Zika represent a major public health problem due to globalization and propagation of susceptible vectors worldwide. Vertebrate host responses to dengue and Zika infections include the processing and release of pro-inflammatory cytokines through the activation of inflammasomes, resulting in disease severity and fatality. Mosquito saliva can facilitate pathogen infection by downregulating the host's immune response. However, the role of mosquito saliva in modulating host innate immune responses remains largely unknown. Here, we show that mosquito salivary gland extract (SGE) inhibits dengue and Zika virus-induced inflammasome activation by reducing NLRP3 expression, Caspase-1 activation, and 1L-1β secretion in cultured human and mice macrophages. As a result, we observe that SGE inhibits virus detection in the early phase of infection. This study provides important insights into how mosquito saliva modulates host innate immunity during viral infection.

INTRODUCTION

Arthropod-borne viruses (arboviruses) cause nearly one million deaths and account for more than 17% of all infectious disease annually. Therefore, arboviruses impose a significant global health problem worldwide.[1] A combination of climate change, urbanization, and globalization have also contributed to the spread of mosquito vectors. Recent studies have predicted that mosquito-borne diseases caused by dengue (DENV) and Zika virus (ZIKV) could threaten one-half of the world's population by the year 2050.[2] Dengue, with more than 100 million cases and 10,000 deaths, was declared the most prevalent arboviral disease worldwide in 2020.[3,4] ZIKV infections have also arose, making the virus one of the most important flaviviruses worldwide. The ZIKV outbreak in Brazil in 2016 was associated with neurological complications and was declared a public health emergency by the WHO.[5] DENV and ZIKV are single-stranded positive sense RNA viruses that belong to the *Flavivirus* genus of the *Flaviviridae* family.[6,7] These viruses are spread by several species of female mosquitoes, principally *Aedes aegypti* and *Aedes albopictus*.[8,9]

Arboviruses are transmitted to vertebrates from the vector during blood meal acquisition. Mosquitoes insert their mouthparts into the skin, simultaneously releasing virus and saliva at the bite site.[8,10,11] Penetration of the skin by mosquito mouthparts causes tissue injury, activating host hemostatic mechanisms consisting of three branches: vasoconstriction, platelet aggregation, and blood clotting. In addition, the immune system of the host also responds to blood vessel and skin tissue injury by creating an acute inflammatory response characterized by swelling, pain, and redness at the injury site.[12,13] Mosquitoes, as well as other blood-feeding arthropods, have evolved a diverse and complex pharmacological repertoire in their saliva known to inhibit both host hemostasis and immune responses, facilitating the acquisition of a blood meal.[12,14,15] Furthermore, mosquito saliva can affect the course of infection, replication capacity of the virus, and host antiviral immune responses.[10,16,17] Previous studies observed that salivary proteins modulate host innate immune responses by downregulating interferons (IFNs) and other proinflammatory cytokines during arbovirus infection such as DENV and ZIKV.[16] The exact mechanism, however, remains unknown.

One of the most important components of innate immune responses is represented by inflammasomes. Inflammasomes are multiprotein complexes consisting of an NLR (NOD-like receptor), the adaptor protein ASC (apoptosis-associated speck-like protein containing a caspase recruitment domain), and the effector protein pro-caspase-1.[18,19] Inflammasomes mediate the initial immune response to pathogens and cellular damage; once activated, they facilitate cleavage and activation of caspase-1, which in turn leads to cleavage of the proinflammatory cytokines interleukin IL-1β and IL-18 into their active form, causing pyroptosis.[19–22]

NLRP3 (NOD-, LRR- and pyrin domain-containing protein 3) inflammasomes play a crucial role in host immune defenses against bacterial, fungal, and viral infections, along with several inflammatory and autoinflammatory diseases.[23,24] In arbovirus infections, the NLRP3 inflammasome induces host inflammatory responses, resulting in IL-1β secretion and disease severity.[25–37]

[1]Laboratory of Malaria and Vector Research, National Institute of Allergy and Infectious Diseases, National Institutes of Health, 12735 Twinbrook Parkway Room 2W09, Bethesda, MD, USA
[2]Lead contact
*Correspondence: ecalvo@niaid.nih.gov
https://doi.org/10.1016/j.isci.2023.108620

Zika virus (ZIKV) infection causes the release of IL-1β including patients, human peripheral blood mononuclear cells (PBMCs) macrophages, mice and mouse bone marrow derived cells (BMDCs). The importance of NLRP3 in this process is evident from experiments where its expression in cells is hindered or genetically removed in mice. As a result, the secretion of IL-1β induced by ZIKV is blocked, highlighting the role of NLRP3.[32] Additionally, the study suggests that the ZIKV NS5 protein plays a role in activating NLRP3 and facilitating the formation of the inflammasome through its interaction with NLPR3 protein, which is essential for IL-1β secretion.[32] Another research emphasizes that ZIKV can trigger responses and elevate levels of IL-1β in various organs such as the brain, spleen, liver and kidney. The activation of NLRP3 inflammasome and involvement of ZIKV non-structural protein 5 (NS5) protein are identified as contributors to this process.[33] Furthermore, it has been observed that ZIKV infection suppresses the expression of IFN-α and a gene called MxA in monocytes. Inhibition of inflammasomes leads to an accumulation of IFNα and IFN inducible genes, within ZIKV infected cells. This suggests that blocking inflammasomes could potentially restore the IFN- dependent antiviral state in ZIKV infected cells.[34] Moreover, a different research study has shown that infection with the ZIKV lead to acute kidney damage, *in vivo* by triggering the inflammasome and apoptosis while also reducing the expression of Bcl-2 [36]. Another study suggests that ZIKV-induced inflammasome activation exacerbate the neuroinflammatory response, consequently increasing damage to the central nervous system (CNS) in neonates with fetal neural ZIKV infection and microcephaly.[38]

Dengue infection is characterized by a spectrum of clinical manifestations, including sudden-onset fever, hepatosplenomegaly, headache, and joint and muscle pain. This fever onset is precipitated by the elevated levels of endogenous pyrogens, such as IL-1β and TNF-α, indicating that Dengue Virus (DENV) infection triggers a robust pyrogenic response in afflicted individuals.[39,40] Notably, DENV exhibits higher replicative efficiency in GM-Mφ, which are inflammatory macrophages characterized by elevated expression levels of C-Type lectin domain containing 5A (CLEC5A), mannose receptor, and NLRP3. This preference for GM-Mφ leads to the activation of the NLRP3 inflammasome, caspase-1 activation, and subsequent release of IL-1β and IL-18. These pro-inflammatory cytokines play a pivotal role in driving fever, increasing vascular permeability, and orchestrating immune responses.[31,41] Further, inhibiting CLEC5A effectively mitigates NLRP3 inflammasome activation, resulting in a reduction in the severity of clinical symptoms.[41,42] Moreover, DENV infection induce pyroptosis, an inflammatory form of cell death primarily mediated by caspase-1 activation through inflammasomes. This pyroptotic process leads to cellular damage and lysis, consequently releasing inflammatory cytokines and further exacerbating the immune response.[43,44] During secondary dengue infection, the phenomenon of antibody-dependent enhancement (ADE) has been proposed as a mechanism for cytokine storms. ADE triggers the secretion of IL-1β in monocytes, mediated by caspase-1 activation, thereby exacerbating the severity of dengue infection.[45,46]

In addition to its role in inflammation, inflammasome activation extends its influence on the adaptive immune response during DENV infection. IL-1β and IL-18, released because of inflammasome activation, play a pivotal role in fostering adaptive immune responses. These cytokines stimulate Th17/γδ T cells, which, in turn, promote the production of pro-inflammatory cytokines, actively contributing to host immune responses.[31,47]

Furthermore, various DENV viral proteins, including EDIII, NS1, NS2A, and NS2B, have been implicated in inflammasome activation. These viral proteins can trigger inflammasomes, leading to the release of pro-inflammatory cytokines and intensifying the immune response against DENV infection.[37] However, the effect of mosquito saliva on inflammasome activation during flavivirus infection remains to be described.

Here we demonstrate that, *Ae. aegypti* salivary gland extracts (*Ae. aegypti* SGE) are associated with a remarkable capacity for inhibiting inflammasome activation, which subsequently reduces downstream caspase-1 activation, IL-1β secretion and cell death during DENV and ZIKV infection in macrophage cells. Importantly, *Ae. aegypti* SGE downregulated NLRP3 expression triggered by DENV and ZIKV infection. We also show that *Ae. aegypti* SGE downregulates gene expression of key innate immune signaling molecules important for DENV and ZIKV recognition, infection, and subsequent inflammasome activation. Taken together, we found that *Ae. aegypti* SGE is key in modulating innate immunity during DENV and ZIKV infection. Our results may further help in the development of drugs with pan-viral activities.

RESULTS

Aedes aegypti SGE reduces inflammasome during DENV and ZIKV infection in human macrophages

Various *Ae. aegypti* salivary proteins have been shown to modulate innate immune responses during flavivirus infections.[16] However, the role of salivary gland extracts or saliva (the vehicle of naturally occurring transmission) in modulating the innate immunity, including inflammasome activation, remains elusive thus far. Because macrophages modulate innate immune responses to mosquito bites and DENV and ZIKV infection, we evaluated the role of *Ae. aegypti* SGE in inflammasome modulation. First, we found that DENV or ZIKV infection induced NLRP3 protein expression (∼118 kDa) when compared to untreated cells. However, *Ae. aegypti* SGE did not show any effect on inflammasome activation. Interestingly, when cells were infected with DENV or ZIKV in the presence of *Ae. aegypti* SGE, the expression of NLRP3 was significantly reduced in the cell lysates (Figures 1A and S1). We also measured secreted active Caspase-1 (∼20 kDa) and IL-1β protein expression (∼17 kDa) in cell supernatants. Cells infected with DENV or ZIKV triggered Caspase-1 activation and IL-1β when compared to untreated cells or those treated only with *Ae. aegypti* SGE. Adding *Ae. aegypti* SGE downregulated Caspase-1 activation and IL-1β in cell supernatants during DENV and ZIKV infection (Figure 1A). To confirm the Western blot results, cell supernatants were also analyzed with Caspase-1 Glo. DENV and ZIKV infection triggered caspase-1 activation and secretion in cell supernatants when compared to control cells or those treated with *Ae. aegypti* SGE alone (Figure 1B). However, *Ae. aegypti* SGE downregulated caspase-1 activation and secretion in cell supernatant during DENV and ZIKV infection. To determine the role of *Ae. aegypti* SGE in regulating pro-inflammatory cytokines, cell supernatants were analyzed by ELISA. for IL-1β, IL-6, IL-8, and IL-18. DENV and ZIKV infection induced robust secretion of IL-1β, (Figure 1C) along with IL-6, IL-8, and IL-18 in cell supernatants as compared to untreated cells or those treated only with *Ae. aegypti* SGE (Figures 1D–1F). Furthermore, a parallel experiment was conducted using primary epidermal keratinocytes (HEKn) from normal human neonatal foreskin, revealing a comparable

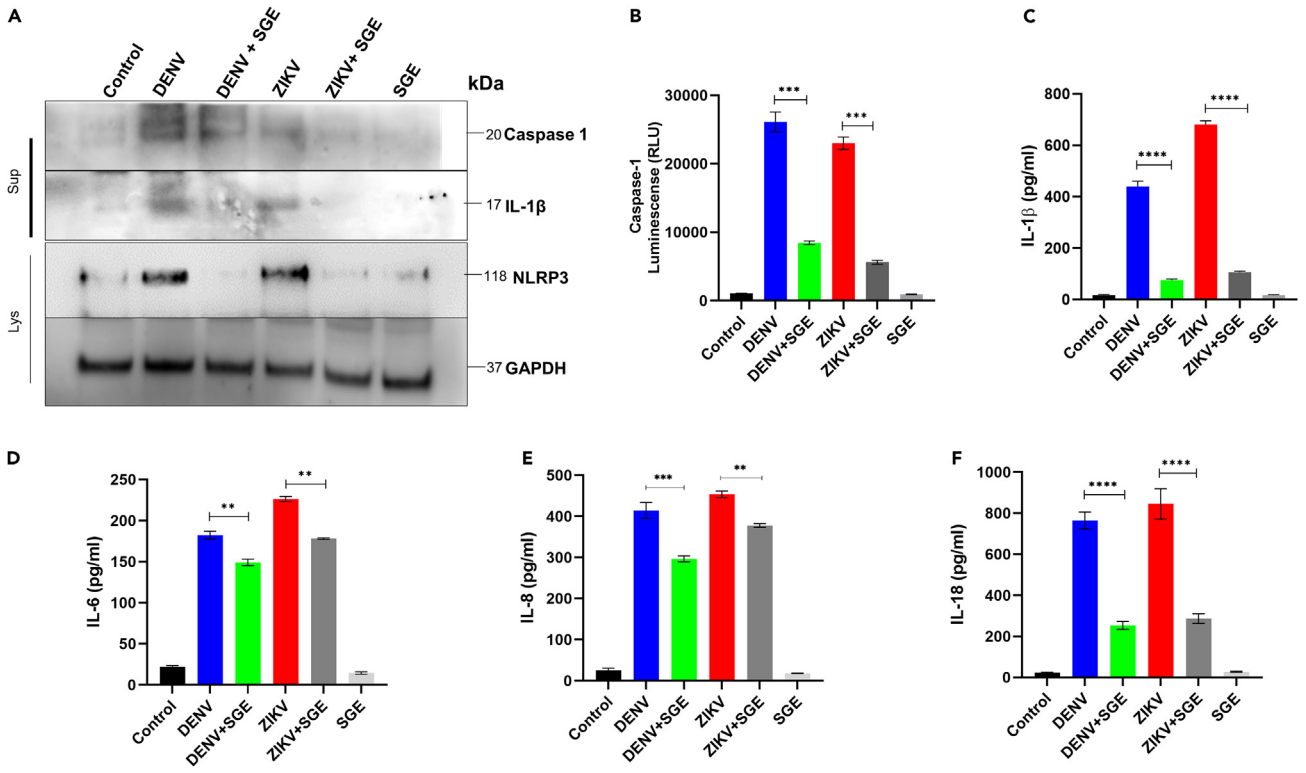

Figure 1. *Aedes aegypti* salivary gland extract (SGE) inhibits DENV or ZIKV-induced inflammasome activation in human macrophages

PMA-primed THP-1 cells were infected with DENV (5 MOI), DENV (5 MOI) + *Ae. aegypti* SGE (2 pairs), ZIKV (5 MOI), ZIKV (5 MOI) + *Ae. aegypti* SGE (2 pairs), *Ae. aegypti* SGE (2 pairs) or left untreated for 36 h.

(A) Secretion of mature IL-1β and cleaved caspase-1 in the supernatants and cell lysate expression of NLRP3 were assessed by Western blot.

(B–F) (B) Active caspase-1 was analyzed by caspase-1 Glo assay. IL-1β (C), IL-6 (D), IL-8 (E), and IL-18 (F) secretions were measured by ELISA. One-way ANOVA with Tukey's multiple comparisons were performed. ****p < 0.0001., ***p < 0.001., **p < 0.01. Molecular weights are indicated in kDa. Data from three independent experiments performed in triplicate are plotted.

impact of *Ae. aegypti* SGE in suppressing the inflammasome. This effect was characterized by reduced Caspase-1 activation and decreased IL-1β secretion during DENV and ZIKV infections (Figure S2). Taken together, these results demonstrate that *Ae. aegypti* SGE reduces NLRP3 inflammasomes in DENV and ZIKV infected-macrophages by inhibiting NLPR3 protein expression, Caspase-1 activation, and pro-inflammatory cytokine release including IL-1β and IL-18 (markers of inflammasomes).

Aedes. aegypti SGE reduces inflammasome during DENV and ZIKV infection in murine macrophages

To corroborate the effect of *Ae. aegypti* SGE on inflammasome activation during DENV and ZIKV infection in human macrophages (THP-1), we tested ASC-expressing RAW 264.7 cells (murine macrophages). RAW 264.7 cells were infected with either DENV or ZIKV alone or with *Ae. aegypti* SGE. Untreated cells (medium) were used as control. Cell supernatants were analyzed with Caspase-1 Glo assay to determine the active caspase-1 and ELISA for IL-1β. As expected, DENV and ZIKV infection triggered caspase-1 activation. No significant effect was found in cells treated with *Ae. aegypti* SGE alone. However, *Ae. aegypti* SGE significantly reduced caspase-1 activation and secretion in cell supernatants during DENV or ZIKV infection (Figure 2A). Similarly, DENV or ZIKV infection stimulated IL-1β secretion as compared to the control group or cells treated with *Ae. aegypti* SGE alone. In addition, *Ae. aegypti* SGE repressed IL-1β secretion in cell supernatants during DENV or ZIKV infection. LPS + Nigericin treatment was used as a positive control of inflammasome activation (Figure 2B). Nigericin, a potassium ionophore, activates NLRP3 inflammasome through the intracellular potassium (K+) efflux across the membrane.[48] Interestingly, *Ae. aegypti* SGE reduced LPS-Nigericin induced inflammasome (Caspase-1 activation and IL-1β secretion) suggesting a potential role of *Ae. aegypti* SGE in regulating potassium efflux (Figure S3). These results confirm the role of *Ae. aegypti* SGE in reducing inflammasome activation during DENV or ZIKV infection in human and murine macrophages.

Aedes. aegypti SGE reduces mitochondrial ROS during DENV or ZIKV infection

The mitochondria plays a pivotal role in the initiation and regulation of the NLRP3 inflammasome during DENV and ZIKV infection, which affects virus replication, cell death, and host immunity.[33,37,49–54] Specifically, several studies unveiled the role of mitochondrial ROS in fueling

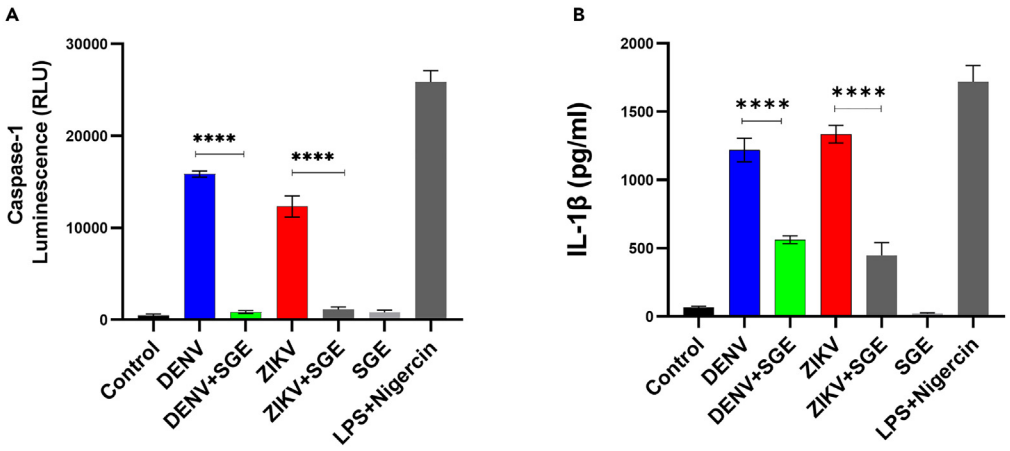

Figure 2. *Aedes aegypti* salivary gland extract (SGE) inhibits DENV or ZIKV-induced inflammasome activation in murine macrophages

RAW-ASC cells (ASC-expressing murine macrophages) were primed with Pam3CSK4 and infected with DENV (5 MOI), DENV (5 MOI) + SGE (2 pairs), ZIKV (5 MOI), ZIKV (5 MOI) + SGE (2 pairs), SGE (2 pairs), or were left untreated for 36 h. As a positive control, cells were treated with LPS (100 ng/mL) for 6 h followed by Nigericin (10 μM) for 24 h.

(A) Active caspase-1 was analyzed by caspase-1 Glo assay.

(B) IL-1β secretions were measured by ELISA. Data from three independent experiments performed in triplicate are plotted. One-way ANOVA with Tukey's multiple comparisons were performed. ****$p < 0.0001$.

NLRP3 inflammasome activation during DENV and ZIKV infections.[55–58] Therefore, to determine the role of *Ae. aegypti* SGE in mitochondrial ROS generation, THP-1 cells were infected with either DENV or ZIKV alone or alongside *Ae. aegypti* SGE or were treated with *Ae. aegypti* SGE only. DENV or ZIKV infection triggered mitochondrial ROS production when compared to the control group or cells treated with *Ae. aegypti* SGE alone (Figure 3A). Rotenone was used as positive control for mitochondrial ROS generation. Rotenone induces the formation of ROS by inhibiting the electron transfer from iron-sulfur centers to ubiquinone in the mitochondrial respiratory chain complex.[59] Mitotempo, a mitochondria-targeted superoxide dismutase cell permeable antioxidant, eliminates mitochondrial superoxide, serves as negative control.[60] We found that *Ae. aegypti* SGE reduced mitochondrial ROS in DENV or ZIKV infected cells, but not in Rotenone induced ROS generation. (Figure S4). These results demonstrate that, *Ae. aegypti* SGE may affect inflammasome activation and DENV and ZIKV pathogenesis by reducing mitochondrial ROS production.

Aedes aegypti SGE reduces virus-mediated inflammasome activation via NLRP3 gene regulation

NLRP3-dependent inflammasomes are activated during DENV and ZIKV infection and modulate antiviral responses that mediate the severity of the pathogenesis.[31,33,37,61] To investigate whether DENV or ZIKV-induced secretion of IL-1β is inflammasome dependent, THP-1 cells were pre-treated with either caspase-1 inhibitor (Ac-YVAD-cmk) or NLRP3 inhibitor (MCC50) and infected with DENV (5 MOI) or ZIKV (5 MOI) or were left untreated. Caspase-1 inhibitor (Ac-YVAD-cmk) and NLRP3 inhibitor (MCC50) significantly reduced IL-1β secretion as compared to DENV or ZIKV infection alone (Figure S5A). These results confirm that secretion of IL-1β during DENV or ZIKV infection is inflammasome dependent in THP-1 cells. Further, we investigated the effect of *Ae. aegypti* SGE in NLRP3-dependent inflammasome activation in THP-1 wild type (WT) andNLRP3 KO THP-1 cells infected with either DENV or ZIKV alone or alongside *Ae. aegypti* SGE. Untreated cells were used as control group. *Aedes aegypti* SGE had no effect on caspase-1 activation or IL-1β secretion during DENV or ZIKV infection in NLRP3 KO THP-1cells as compared to THP-1 WT cells (Figures 4A–4D). These results demonstrate the role of *Ae. aegypti* SGE in modulating inflammasome activation through the NLRP3 pathway. The validation of NLRP3 KO THP-1 was performed by treating NLRP3 KO THP-1 and THP-1 WT cells with LPS and ATP (inducers of inflammasome) and subsequent quantification of NLRP3 expression (Figure S5B), caspase-1 activation (Figures S5C and S5D), and secretion of IL-1β and IL-18 (Figures S5E and S5F).

Aedes aegypti SGE rescues cell death without affecting replication during DENV or ZIKV infection

We studied the effect of *Ae. aegypti* SGE in cell death during DENV or ZIKV infection. *Ae. aegypti* SGE rescued the cell death caused by DENV or ZIKV infection as compared to DENV and ZIKV infection alone. No effect was observed in cells treated with *Ae. aegypti* SGE alone. As a positive control, cells were treated with LPS + ATP as well as Triton X-100 (Figure 5A). Our results indicate that, *Ae. aegypti* SGE leads to decreased pathogenesis by inhibiting cell death. To determine the effect of *Ae. aegypti* SGE on DENV and ZIKV infection in THP-1 cells, cells were infected with either DENV or ZIKV alone or alongside *Ae. aegypti* SGE, or they were left untreated for 24 h. Infectious virus titers were quantified in cell supernatants by plaque assay. *Ae. aegypti* SGE had no effect on DENV or ZIKV replication *in vitro* (THP-1 cells) (Figure 5B). In addition to plaque assay, DENV NS5 and ZIKV NS5 gene expression was analyzed by RT-PCR. No effect of *Ae. aegypti* SGE on DENV or ZIKV infection in THP-1 cells was found (Figures S6A and S6B).

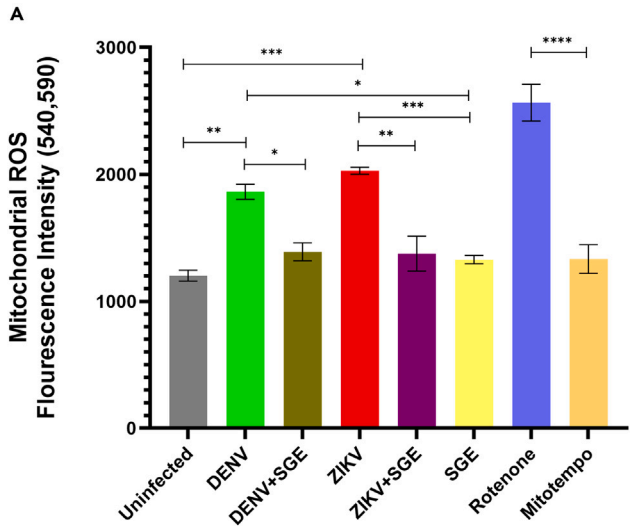

Figure 3. *Aedes aegypti* salivary gland extract (SGE) inhibits DENV or ZIKV-triggered mitochondrial ROS in human macrophages

PMA primed THP-1 cells were infected with DENV (5 MOI), DENV (5 MOI) + SGE (2 pairs), ZIKV (5 MOI), ZIKV (5 MOI) + SGE (2 pairs), SGE (2 pairs) or were left untreated for 36 h in 96 well black wall/clear bottom plate. Cells were treated with rotenone (positive control, 10 μM) for 3 h or Mitotempo (negative control, 500 μM) for 60 min at 37°C. Cells were then incubated with MitoROS 580 at 37°C for 1 h. The fluorescence signal was monitored at Ex/Em = 485/535 nm with bottom read mode using a microplate reader. Data from three independent experiments performed in triplicate are plotted. One-way ANOVA with Tukey's multiple comparisons were performed. ****p < 0.0001, ***p < 0.001, **p < 0.01, *p < 0.05.

Aedes aegypti SGE downregulates innate immune and antiviral genes

Mosquito salivary glands harbor several pharmacologically active compounds that can modulate virus infection, replication, and host innate immune responses.[10,17,62] To observe the effect of *Ae. aegypti* SGE on innate immune regulation during DENV and ZIKV infection, THP-1 WT cells were infected with either DENV or ZIKV alone or alongside *Ae. aegypti* SGE, or they were left untreated for 24 h. The presence of *Ae. aegypti* SGE with DENV downregulated the mRNA expression of human *TLR-3, IRF-3, NF-kB, RelA, NLRP3, AIM2, caspase-1, IFN-β, SYK, STAT-1, MX1, OAS2, CXCL10, CXCL11,* and *DDX58* (Figures 6A, 6B, and S7). Similarly, the presence of *Ae. aegypti* SGE with ZIKV downregulated the mRNA expression of human *TLR-3, IRF-3, NF-kB, RelA, NLRP3, AIM2, caspase-1, IFN-β, SYK, STAT-1, CXCL10,* and *CXCL11* (Figures 6A, 6B, and S7).

Aedes aegypti SGE downregulates early host innate response induced by DENV and ZIKV infection

To determine the role of *Ae. aegypti* SGE in early innate immune responses at the translational level, we chose some of the genes (*NF-kB-P65, NF-kB-P50, SYK, STAT-1,* and *IRF-3*) that play crucial roles in early DENV and ZIKV infection sensing and early innate immune signaling cascades. The presence of *Ae. aegypti* SGE during DENV or ZIKV infection downregulated phosphorylated protein expression of human NF-kB-P50, NF-kB-P65, SYK, STAT-1, and IRF-3 in THP-1 macrophages (Figure 7). Taken together, these results demonstrate the key role of *Ae. aegypti* SGE in downregulating transcriptional and translation expression of key innate immune response players. This downregulation might provide an additive benefit for the virus to evade host innate immune responses and efficiently proliferate in host cells.

DISCUSSION

During DENV and ZIKV infection, host immune cells recognize PRRs (pathogen recognition receptors) and trigger host innate immunity, including production of cytokines and chemokines and interferon responses, which subsequently induces an antiviral state.[63–68] NLRP3 is an intracellular sensor that detects a diverse range of pathogen-associated molecular patterns (PAMPs) and danger-associated molecular patterns (DAMPs) generated during viral infection that activate NLRP3 inflammasome-dependent antiviral immune responses.[18,24,69,70] The NLRP3 inflammasome is triggered by many families of viruses, suggesting a common pathway for viral detection and response by the host cell.[18,71]

The NLRP3-dependent inflammasome is activated during DENV and ZIKV infection and modulates antiviral responses, resulting in disease severity.[31,33,37,61] Various pharmacologically active compounds with the capacity to manipulate virus infection, replication, and the host's innate immune response are present in mosquito salivary glands.[10,17,62] However, the role of salivary gland extracts and saliva (the vehicle of naturally occurring transmission) in modulating the innate immune response, including inflammasome activation, remains elusive thus far.

In this manuscript, we have demonstrated that SGE downregulates the NLRP3 inflammasome activation by inhibiting NLRP3 protein expression, which leads to the subsequent downregulation of caspase-1 activation, and inflammatory cytokine release (IL- 1β, IL-6, IL-8, and IL-18). Given the various DAMPs that affect inflammasome activation, mitochondria have been reported to play pivotal role in initiation and regulation of the NLRP3 inflammasome during DENV and ZIKV infection, which affects virus replication, cell death, and host immunity.[33,49–54,72] Previous work unveiled the role of mitochondrial ROS in fueling NLRP3 inflammasome activation during DENV and ZIKV

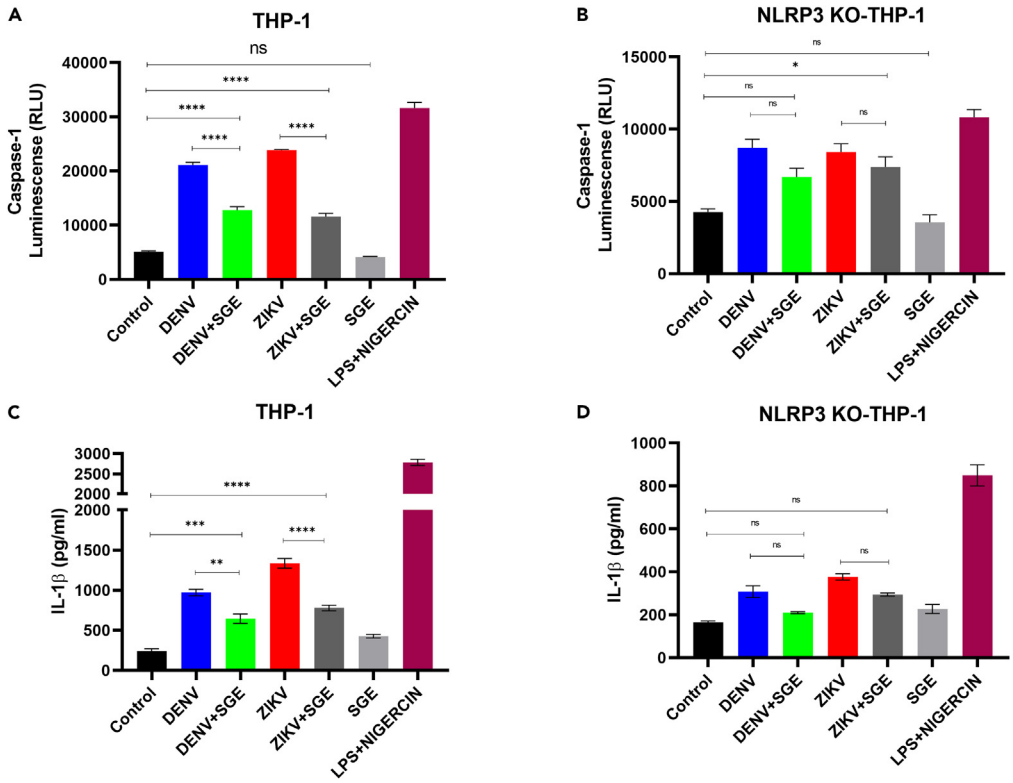

Figure 4. NLRP3 plays a crucial role in *Ae aegypti* salivary gland extract (SGE)-mediated reduction of inflammasome activation

(A–D) PMA-primed THP-1 and NLRP3 KO THP-1 cells were infected with DENV (5 MOI), DENV (5 MOI) + SGE (2 pairs), ZIKV (5 MOI), ZIKV (5 MOI) + SGE (2 pairs), SGE (2 pairs), or were left untreated for 36 h. Subsequently, we assessed the activation of caspase-1 using the caspase-1 Glo assay (A and B). Secretion of mature IL-1β was assessed by ELISA (C and D). Data from three independent experiments performed in triplicate are plotted. One-way ANOVA with Tukey's multiple comparisons were performed. ****$p < 0.0001$., **$p < 0.01$., ns, not significant.

infections.[55–58] We showed the role of *Ae. aegypti* SGE in downregulating mitochondrial ROS, a DAMP inhibitor for NLRP3 activation, during DENV or ZIKV infection.

Once the host innate immune system senses conserved microbial molecules during pathogen infection, many cells rapidly respond by generating inflammatory mediators and initiating programmed cell death pathways comprised of pyroptosis, apoptosis, and necroptosis.[73] A growing body of evidence has demonstrated the induction of apoptosis and pyroptosis during DENV infection in human monocytes and macrophages. Similarly, ZIKV infection induces cell death via apoptosis and pyroptosis, which inhibits the development of human neural progenitor cells and leads to microcephaly.[38,74–76] *In vivo, Ae. aegypti* saliva was found to affect DENV and ZIKV replication in rhesus macaques. Bites from DENV-infected mosquitoes resulted in higher viremia when compared with DENV alone or DENV + *Ae. aegypti* SGE.[77] Similarly, ZIKV inoculation via mosquito bite resulted in systemic infection and altered tissue tropism as compared to ZIKV inoculation via subcutaneous needle in rhesus macaques.[78] Another study demonstrated a protein specific to mosquito saliva, designated as *Ae. aegypti* venom allergen-1 (AaVA-1), enhances the transmission of dengue and Zika viruses by initiating autophagy in host immune cells belonging to the monocyte lineage.[79] We demonstrate the effect of *Ae. aegypti* SGE in rescuing the cell death caused by DENV or ZIKV as compared to DENV or ZIKV alone without affecting replication.

During viral infection, PRR engagement leads to the activation of interferon regulatory factor 3 (IRF-3), interferon regulatory factor 7 (IRF-7) I and NF-κB, which further trigger transcription and secretion of IFNs and inflammatory cytokines. The IFNs, by binding to their receptors (IFNAR), activate Janus kinase (Jak)/Signal transducer and activator of transcription (STAT), which leads to the induction of interferon stimulated genes (ISGs). ISGs hamper different stages of the viral life cycle and create an anti-viral state.[80] Though IFNAR and PRR activation regulate ISGs, ISGs can also be directly triggered by IRF3 in an IFN-independent pathway.[80,81]

DENV and ZIKV transmission to vertebrate hosts occurs when an infected mosquito probes the host's skin in search of a blood meal. Mosquito saliva is known to help blood-feeding and has also been shown to enhance pathogen transmission. Various *Ae. aegypti* salivary proteins have been shown to modulate innate immune responses in flavivirus infections.[16] We observed the role of *Ae. aegypti* SGE in modulating innate immunity during DENV and ZIKV infection. Mosquito *Ae. aegypti* SGE downregulates *TLR-3, IRF-3, NF-kB, RelA, NLRP3, AIM2, Caspase-1, IFN-β, SYK, STAT-1, MX1, OAS2, CXCL10, CXCL11*, and *DDX58* at the mRNA level during DENV infection and *TLR-3, IRF-3, NF-kB, RelA, NLRP3, AIM2, Caspase-1, IFN-β, SYK, STAT-1, CXCL10*, and *CXCL11* during ZIKV, demonstrating the role of *Ae. aegypti* SGE

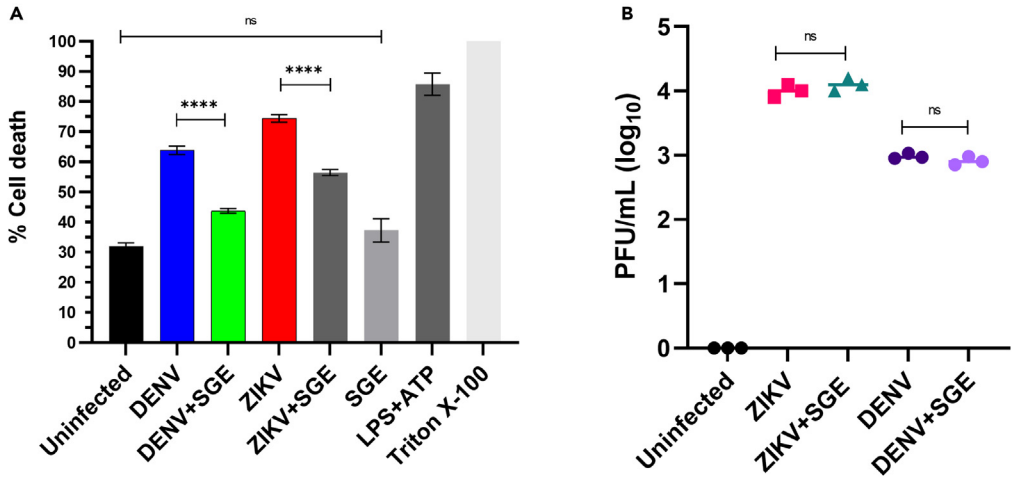

Figure 5. *Aedes aegypti* salivary gland extract (SGE) rescues cell death without effecting DENV or ZIKV replication

(A) PMA-primed THP-1 cells were infected with DENV (5 MOI), DENV (5 MOI) + SGE (2 pairs), ZIKV (5 MOI), ZIKV (5 MOI) + SGE (2 pairs), SGE (2 pairs), or left untreated for 36 h in 96-well black wall/clear bottom plate. As a positive control for inflammasome activation, cells were treated with LPS (100 ng/mL) for 6 h followed by ATP (5 mM) for 1 h. As a positive control for cell death, cells were treated with Triton X-100 for 10 min. All treatments were performed in a medium containing SYTOX Green Nucleic Acid Stain (50 nM). The fluorescence signal was monitored at Ex/Em = 480/530 nm with bottom read mode using a microplate reader. The signals were normalized with controls (wells without cells) and compared with the values of cells treated with Triton X-100, which was considered as 100% cell death.

(B) PMA-primed THP-1 cells were infected with DENV (5 MOI), DENV (5 MOI) + SGE (2 pairs), ZIKV (5 MOI), ZIKV (5 MOI) + SGE (2 pairs), SGE (2 pairs), or were left untreated for 24 h in a 6 well plate. Infected cell supernatants were analyzed by plaque assay to quantify infectious viral particles. Data from three independent experiments performed in triplicate are plotted. One-way ANOVA with Tukey's multiple comparisons were performed. ****p < 0.0001., ns - not significant.

in downregulating PRRs and subsequent signaling cascades. Signaling mechanisms that trigger *IRF3*, *SYK* (as PRRs) and genes related to innate immune pathways, or activation by type I IFNs such as STAT1 and NF-kB, have been shown to play crucial role in DENV sensing and subsequent disease pathogenesis.[45,82–85] In summary, mosquito *Ae. aegypti* SGE inhibits the function of crucial immune proteins and thereby interferes with viral sensing and subsequent downstream pathways during DENV and ZIKV infection as summarized in Figure 8.

Arbovirus infections have created a serious public health problem worldwide. Thus, new approaches are needed to control arbovirus transmission and disease occurrence worldwide. Our work demonstrates the importance of salivary components of arthropods in the pathogenesis of arboviruses.

Limitations of the study

There are several gaps that need to be addressed to understand the complex interactions among host-vector-virus. For example, understanding the mechanisms by which saliva components restructure the local immune response at the bite site can be used in the development of

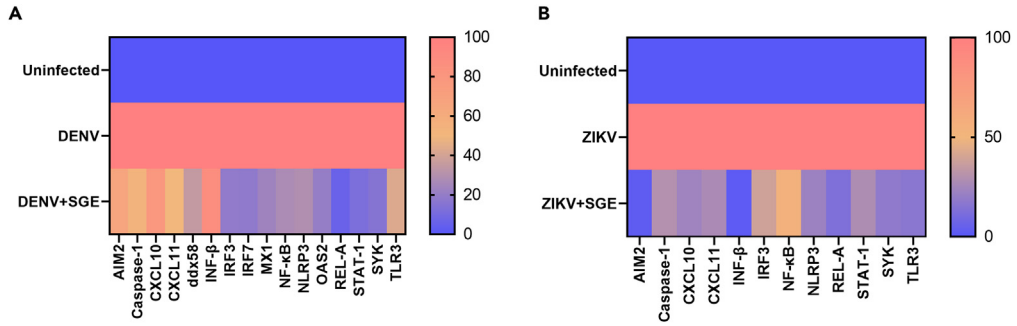

Figure 6. *Aedes aegypti* salivary gland extract (SGE) downregulates mRNA expression of innate immune and antiviral genes during DENV or ZIKV infection

PMA-primed THP-1 cells were infected with DENV (5 MOI), DENV (5 MOI) + SGE (2 pairs), ZIKV (5 MOI), ZIKV (5 MOI) + SGE (2 pairs), SGE (2 pairs), or were left untreated for 24 h. Gene expression was analyzed using RT-qPCR.

(A and B) Heatmap showing the expression patterns of commonly affected genes by DENV and ZIKV infection. Pink and purple represent the upregulated and down regulated genes, respectively. Data from three independent experiments performed in triplicate were normalized and plotted.

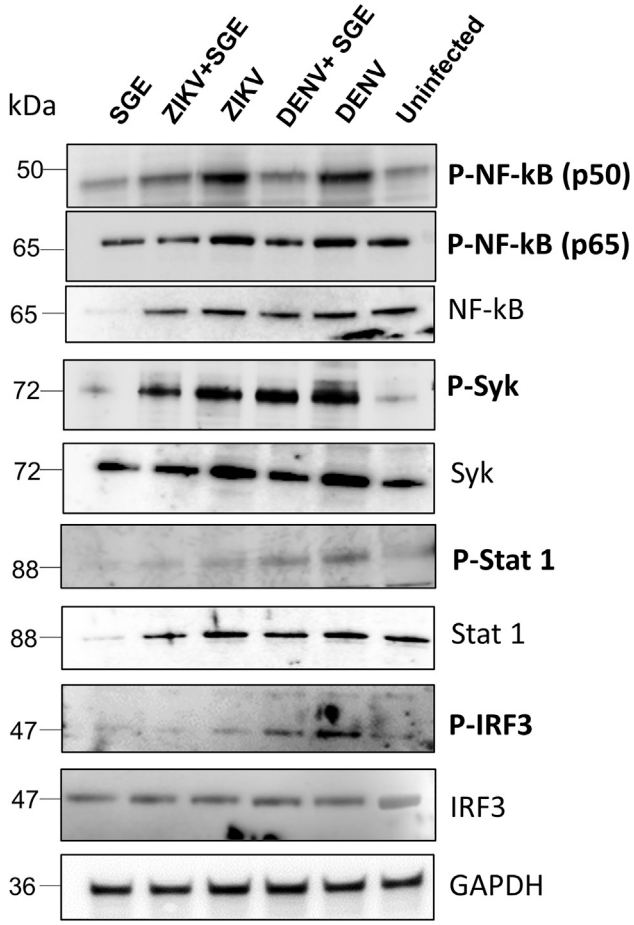

Figure 7. *Aedes aegypti* salivary gland extract (SGE) inhibits early innate immune sensing of DENV and ZIKV infection

PMA-primed THP-1 cells were infected with DENV (5 MOI), DENV (5 MOI) + SGE (2 pairs), ZIKV (5 MOI), ZIKV (5 MOI) + SGE (2 pairs), SGE (2 pairs), or were left untreated for 3 h. Protein expression of total NF-kB-p65, Syk, Stat 1, and IRF3 were assessed along with the phosphorylated forms P-NF-kB-p65, P-NF-kB-p50, P-Syk, P -Stat-1, Stat-1, Phospho (P)- IRF3 in cell lysates by Western blot. GAPDH expression was used as a protein loading control.

interventions against arbovirus infections. In addition, *Ae. aegypti* SGE factors need to be functionally characterized during viral infections, as well as how composition and abundance of salivary compounds are regulated during viral infection. Nevertheless, there is a growing hope for salivary vaccine development as several animal studies are displaying promising outcomes in clinical trials to generate a universal vector vaccine against distinct viral infections. Although we described herein the effects of *Ae. aegypti* SGE on viral infection, the specific factors responsible for these activities remain to be discovered. Future work studying individual salivary proteins may lead to the development of vector-based vaccine against flavivirus infection. An additional constraint of this research lies in the absence of robust *in vivo* model, inclusion of another arbovirus or a virus from different family transmitted by *Ae. aegypti*, as well as the use of saliva instead of SGE, which could provide additional substantiation for the underlying hypothesis of this study. While the data highlights the significance of NLRP3 as a crucial sensor in regulating the inflammasome during SGE-induced responses to dengue and Zika infection, it is plausible that an alternative, NLRP3-independent pathway may also contribute to this intricate interaction. It is imperative to delve into other inflammasome sensors and conduct comprehensive investigations regarding their responses to SGE and viral infections. This approach will enable a more in-depth comprehension of the intricate interplay among mosquitoes, viruses, and their human host.

STAR★METHODS

Detailed methods are provided in the online version of this paper and include the following:

- KEY RESOURCES TABLE
- RESOURCE AVAILABILITY
  - Lead contact
  - Materials availability

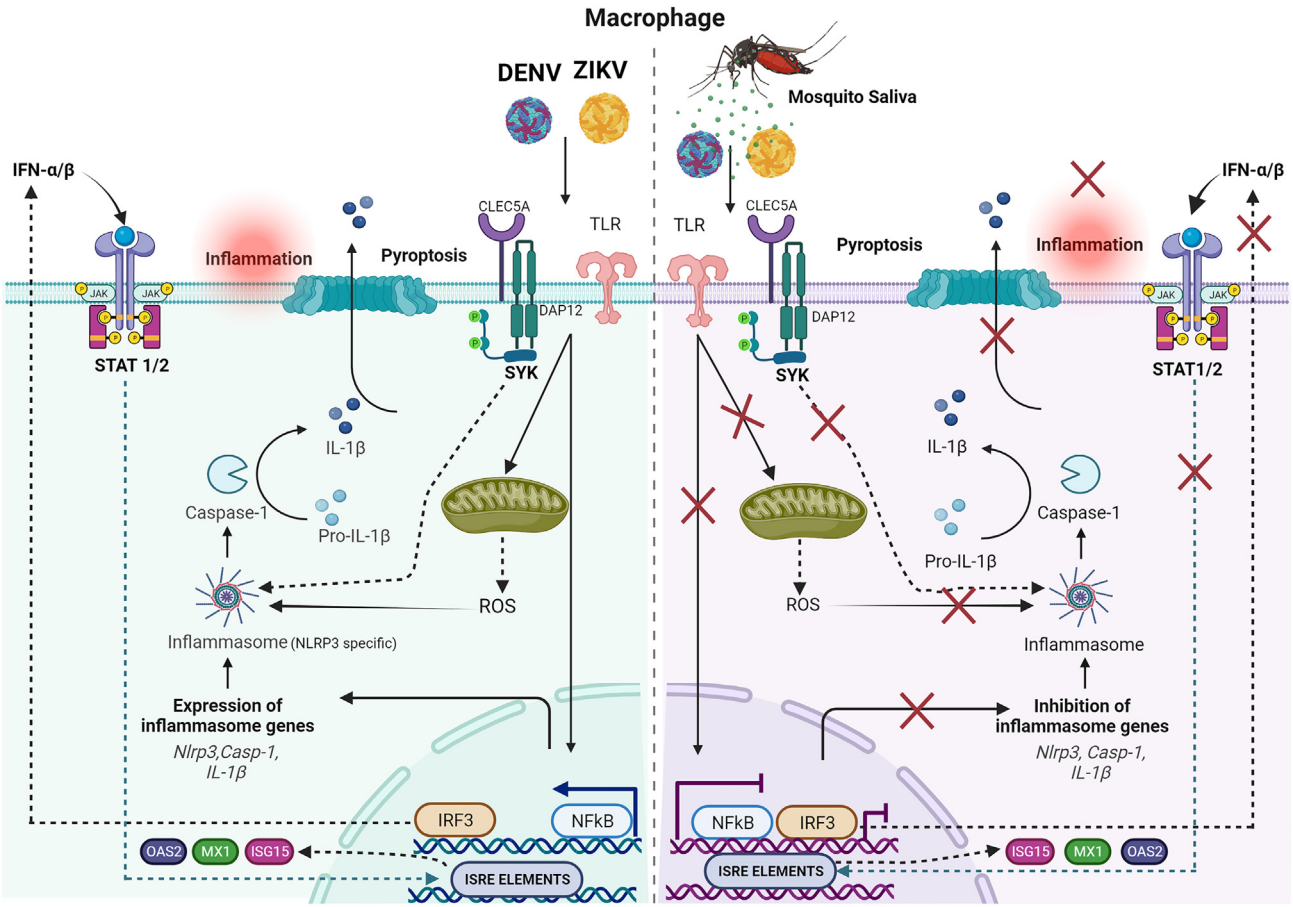

Figure 8. Schematic representation of *Ae aegypti* salivary gland extract (SGE) effects on innate immune responses during DENV and ZIKV infection

In macrophages, DENV and ZIKV infection induce inflammasome activation along with the expression of genes that modulate the antiviral response. However, during a blood meal, mosquito injects salivary proteins and viral particles into the vertebrate host's skin. Mosquito saliva from *Ae. aegypti* interferes with innate immune responses and changes the host antiviral response against DENV and ZIKV. As the viral particles enter into the host skin, mosquito saliva downregulates SYK, NF-kB, IRF3, and STAT-1 protein expression in the early stages of viral infection in macrophages (3 h). Subsequently, it proceeds to inhibit the activation of the inflammasome, effectively suppressing NLRP3 protein expression, IL-1β secretion, caspase-1 activation, and mitigating mitochondrial ROS generation. These actions collectively contribute to a reduction in cell death triggered by DENV and ZIKV infection.

SUPPLEMENTAL INFORMATION

Supplemental information can be found online at https://doi.org/10.1016/j.isci.2023.108620.

ACKNOWLEDGMENTS

The authors thank Dr. Adeline E. Williams (NIAID) and Yolanda L. Jones, NIH Library Editing Services, for manuscript editing assistance. We also thank Dr. Ian Fraser, NIAID, for critical evaluation of this work and to Mr. Brian Bonilla for mosquito rearing and salivary gland dissections. Funding This research was supported by the Division of Intramural Research Program of the NIH/NIAID, United States (AI001246). Because the authors are government employees and this is a government work, the work is in the public domain in the United States. Notwithstanding any other agreements, the NIH reserves the right to provide the work to PubMed Central for display and use by the public, and PubMed Central may tag or modify the work consistent with its customary practices. You can establish rights outside of the US subject to a government use license.

AUTHOR CONTRIBUTIONS

Conceptualization, E.C. and G.S.; methodology, E.C., G.S., and P.C.V-L.; formal analysis, E.C., G.S., and P.C.V.-L.; investigation, G.S., P.C.V-L., and K.B.; writing—original draft preparation, G.S.; writing—review and editing, E.C., G.S., P.C.V-L., and K.B.; All authors have read and agreed to the final version of the manuscript.

DECLARATION OF INTERESTS

The authors declare no competing interests.

Received: August 1, 2023
Revised: October 16, 2023
Accepted: November 30, 2023
Published: December 2, 2023

REFERENCES

1. WHO (2020). Vector-borne diseases. https://www.who.int/news-room/fact-sheets/detail/vector-borne-diseases.
2. Kraemer, M.U.G., Reiner, R.C., Jr., Brady, O.J., Messina, J.P., Gilbert, M., Pigott, D.M., Yi, D., Johnson, K., Earl, L., Marczak, L.B., et al. (2019). Past and future spread of the arbovirus vectors Aedes aegypti and Aedes albopictus. Nat. Microbiol. *4*, 854–863.
3. Bhatt, S., Gething, P.W., Brady, O.J., Messina, J.P., Farlow, A.W., Moyes, C.L., Drake, J.M., Brownstein, J.S., Hoen, A.G., Sankoh, O., et al. (2013). The global distribution and burden of dengue. Nature *496*, 504–507.
4. Messina, J.P., Brady, O.J., Golding, N., Kraemer, M.U.G., Wint, G.R.W., Ray, S.E., Pigott, D.M., Shearer, F.M., Johnson, K., Earl, L., et al. (2019). The current and future global distribution and population at risk of dengue. Nat. Microbiol. *4*, 1508–1515.
5. Lupton, K. (2016). Zika virus disease: a public health emergency of international concern. Br. J. Nurs. *25*, 198–200.
6. Fernandez-Garcia, M.D., Mazzon, M., Jacobs, M., and Amara, A. (2009). Pathogenesis of flavivirus infections: using and abusing the host cell. Cell Host Microbe *5*, 318–328.
7. Laureti, M., Narayanan, D., Rodriguez-Andres, J., Fazakerley, J.K., and Kedzierski, L. (2018). Flavivirus Receptors: Diversity, Identity, and Cell Entry. Front. Immunol. *9*, 2180.
8. McCracken, M.K., Christofferson, R.C., Grasperge, B.J., Calvo, E., Chisenhall, D.M., and Mores, C.N. (2014). Aedes aegypti salivary protein "aegyptin" co-inoculation modulates dengue virus infection in the vertebrate host. Virology *468–470*, 133–139.
9. Huang, Y.J., Higgs, S., Horne, K.M., and Vanlandingham, D.L. (2014). Flavivirus-mosquito interactions. Viruses *6*, 4703–4730.
10. Vogt, M.B., Lahon, A., Arya, R.P., Kneubehl, A.R., Spencer Clinton, J.L., Paust, S., and Rico-Hesse, R. (2018). Mosquito saliva alone has profound effects on the human immune system. PLoS Neglected Trop. Dis. *12*, e0006439.
11. Fong, S.W., Kini, R.M., and Ng, L.F.P. (2018). Mosquito Saliva Reshapes Alphavirus Infection and Immunopathogenesis. J. Virol. *92*.
12. Martin-Martin, I., Smith, L.B., Chagas, A.C., Sá-Nunes, A., Shrivastava, G., Valenzuela-Leon, P.C., and Calvo, E. (2020). Aedes albopictus D7 Salivary Protein Prevents Host Hemostasis and Inflammation. Biomolecules *10*.
13. Ribeiro, J.M., and Francischetti, I.M. (2003). Role of arthropod saliva in blood feeding: sialome and post-sialome perspectives. Annu. Rev. Entomol. *48*, 73–88.
14. Arcà, B., and Ribeiro, J.M. (2018). Saliva of hematophagous insects: a multifaceted toolkit. Curr. Opin. Insect Sci. *29*, 102–109.
15. Mans, B.J. (2011). Evolution of vertebrate hemostatic and inflammatory control mechanisms in blood-feeding arthropods. J. Innate Immun. *3*, 41–51.
16. Guerrero, D., Cantaert, T., and Missé, D. (2020). Aedes Mosquito Salivary Components and Their Effect on the Immune Response to Arboviruses. Front. Cell. Infect. Microbiol. *10*, 407.
17. Schneider, B.S., and Higgs, S. (2008). The enhancement of arbovirus transmission and disease by mosquito saliva is associated with modulation of the host immune response. Trans. R. Soc. Trop. Med. Hyg. *102*, 400–408.
18. Shrivastava, G., León-Juárez, M., García-Cordero, J., Meza-Sánchez, D.E., and Cedillo-Barrón, L. (2016). Inflammasomes and its importance in viral infections. Immunol. Res. *64*, 1101–1117.
19. Platnich, J.M., and Muruve, D.A. (2019). NOD-like receptors and inflammasomes: A review of their canonical and non-canonical signaling pathways. Arch. Biochem. Biophys. *670*, 4–14.
20. Broz, P., and Dixit, V.M. (2016). Inflammasomes: mechanism of assembly, regulation and signalling. Nat. Rev. Immunol. *16*, 407–420.
21. Shi, J., Zhao, Y., Wang, K., Shi, X., Wang, Y., Huang, H., Zhuang, Y., Cai, T., Wang, F., and Shao, F. (2015). Cleavage of GSDMD by inflammatory caspases determines pyroptotic cell death. Nature *526*, 660–665.
22. Rathinam, V.A., and Fitzgerald, K.A. (2016). Inflammasome Complexes: Emerging Mechanisms and Effector Functions. Cell *165*, 792–800.
23. Fusco, R., Siracusa, R., Genovese, T., Cuzzocrea, S., and Di Paola, R. (2020). Focus on the Role of NLRP3 Inflammasome in Diseases. Int. J. Mol. Sci. *21*.
24. Kelley, N., Jeltema, D., Duan, Y., and He, Y. (2019). The NLRP3 Inflammasome: An Overview of Mechanisms of Activation and Regulation. Int. J. Mol. Sci. *20*.
25. Shrivastava, G., Visoso-Carvajal, G., Garcia-Cordero, J., Leon-Juarez, M., Chavez-Munguia, B., Lopez, T., Nava, P., Villegas-Sepulveda, N., and Cedillo-Barron, L. (2020). Dengue Virus Serotype 2 and Its Non-Structural Proteins 2A and 2B Activate NLRP3 Inflammasome. Front. Immunol. *11*, 352.
26. Lien, T.S., Sun, D.S., Wu, C.Y., and Chang, H.H. (2021). Exposure to Dengue Envelope Protein Domain III Induces Nlrp3 Inflammasome-Dependent Endothelial Dysfunction and Hemorrhage in Mice. Front. Immunol. *12*, 617251.
27. Lien, T.S., Chan, H., Sun, D.S., Wu, J.C., Lin, Y.Y., Lin, G.L., and Chang, H.H. (2021). Exposure of Platelets to Dengue Virus and Envelope Protein Domain III Induces Nlrp3 Inflammasome-Dependent Platelet Cell Death and Thrombocytopenia in Mice. Front. Immunol. *12*, 616394.
28. Khan, R.A., Afroz, S., Minhas, G., Battu, S., and Khan, N. (2019). Dengue virus envelope protein domain III induces pro-inflammatory

signature and triggers activation of inflammasome. Cytokine *123*, 154780.
29. Pan, P., Zhang, Q., Liu, W., Wang, W., Lao, Z., Zhang, W., Shen, M., Wan, P., Xiao, F., Liu, F., et al. (2019). Dengue Virus M Protein Promotes NLRP3 Inflammasome Activation To Induce Vascular Leakage in Mice. J. Virol. *93*.
30. Pan, P., Zhang, Q., Liu, W., Wang, W., Yu, Z., Lao, Z., Zhang, W., Shen, M., Wan, P., Xiao, F., et al. (2019). Dengue Virus Infection Activates Interleukin-1β to Induce Tissue Injury and Vascular Leakage. Front. Microbiol. *10*, 2637.
31. Wu, M.F., Chen, S.T., and Hsieh, S.L. (2013). Distinct regulation of dengue virus-induced inflammasome activation in human macrophage subsets. J. Biomed. Sci. *20*, 36.
32. Wang, W., Li, G., De, W., Luo, Z., Pan, P., Tian, M., Wang, Y., Xiao, F., Li, A., Wu, K., et al. (2018). Zika virus infection induces host inflammatory responses by facilitating NLRP3 inflammasome assembly and interleukin-1β secretion. Nat. Commun. *9*, 106.
33. He, Z., Chen, J., Zhu, X., An, S., Dong, X., Yu, J., Zhang, S., Wu, Y., Li, G., Zhang, Y., et al. (2018). NLRP3 Inflammasome Activation Mediates Zika Virus-Associated Inflammation. J. Infect. Dis. *217*, 1942–1951.
34. Khaiboullina, S.F., Uppal, T., Sarkar, R., Gorzalski, A., St Jeor, S., and Verma, S.C. (2017). ZIKV infection regulates inflammasomes pathway for replication in monocytes. Sci. Rep. *7*, 16050.
35. Gim, E., Shim, D.W., Hwang, I., Shin, O.S., and Yu, J.W. (2019). Zika Virus Impairs Host NLRP3-mediated Inflammasome Activation in an NS3-dependent Manner. Immune Network *19*, e40.
36. Liu, T., Tang, L., Tang, H., Pu, J., Gong, S., Fang, D., Zhang, H., Li, Y.P., Zhu, X., Wang, W., et al. (2019). Zika Virus Infection Induces Acute Kidney Injury Through Activating NLRP3 Inflammasome Via Suppressing Bcl-2. Front. Immunol. *10*, 1925.
37. Shrivastava, G., Valenzuela Leon, P.C., and Calvo, E. (2020). Inflammasome Fuels Dengue Severity. Front. Cell. Infect. Microbiol. *10*, 489.
38. de Sousa, J.R., Azevedo, R., Martins Filho, A.J., de Araujo, M.T.F., Cruz, E., Vasconcelos, B.C.B., Cruz, A.C.R., de Oliveira, C.S., Martins, L.C., Vasconcelos, B.H.B., et al. (2018). In situ inflammasome activation results in severe damage to the central nervous system in fatal Zika virus microcephaly cases. Cytokine *111*, 255–264.
39. Setiawan, M.W., Samsi, T.K., Wulur, H., Sugianto, D., and Pool, T.N. (1998). Dengue haemorrhagic fever: ultrasound as an aid to predict the severity of the disease. Pediatr. Radiol. *28*, 1–4.
40. Wu, K.L., Changchien, C.S., Kuo, C.H., Chiu, K.W., Lu, S.N., Kuo, C.M., Chiu, Y.C., Chou, Y.P., and Chuah, S.K. (2004). Early abdominal sonographic findings in patients with dengue fever. J. Clin. Ultrasound *32*, 386–388.
41. Wu, M.F., Chen, S.T., Yang, A.H., Lin, W.W., Lin, Y.L., Chen, N.J., Tsai, I.S., Li, L., and Hsieh, S.L. (2013). CLEC5A is critical for dengue virus-induced inflammasome activation in human macrophages. Blood *121*, 95–106.
42. Chen, S.T., Lin, Y.L., Huang, M.T., Wu, M.F., Cheng, S.C., Lei, H.Y., Lee, C.K., Chiou, T.W., Wong, C.H., and Hsieh, S.L. (2008). CLEC5A is critical for dengue-virus-induced lethal disease. Nature *453*, 672–676.
43. Tan, T.Y., and Chu, J.J.H. (2013). Dengue virus-infected human monocytes trigger late activation of caspase-1, which mediates pro-inflammatory IL-1β secretion and pyroptosis. J. General Virol. *94*, 2215–2220.
44. Cheung, K.T., Sze, D.M., Chan, K.H., and Leung, P.H. (2018). Involvement of caspase-4 in IL-1 beta production and pyroptosis in human macrophages during dengue virus infection. Immunobiology *223*, 356–364.
45. Callaway, J.B., Smith, S.A., McKinnon, K.P., de Silva, A.M., Crowe, J.E., Jr., and Ting, J.P. (2015). Spleen Tyrosine Kinase (Syk) Mediates IL-1β Induction by Primary Human Monocytes during Antibody-enhanced Dengue Virus Infection. J. Biol. Chem. *290*, 17306–17320.
46. Kamaladasa, A., Gomes, L., Wijesinghe, A., Jeewandara, C., Toh, Y.X., Jayathilaka, D., Ogg, G.S., Fink, K., and Malavige, G.N. (2019). Altered monocyte response to the dengue virus in those with varying severity of past dengue infection. Antiviral. Res. *169*, 104554.
47. Tsai, C.Y., Liong, K.H., Gunalan, M.G., Li, N., Lim, D.S., Fisher, D.A., MacAry, P.A., Leo, Y.S., Wong, S.C., Puan, K.J., and Wong, S.B. (2015). Type I IFNs and IL-18 regulate the antiviral response of primary human γδ T cells against dendritic cells infected with Dengue virus. J. Immunol. *194*, 3890–3900.
48. Muñoz-Planillo, R., Kuffa, P., Martínez-Colón, G., Smith, B.L., Rajendiran, T.M., and Núñez, G. (2013). K^+ efflux is the common trigger of NLRP3 inflammasome activation by bacterial toxins and particulate matter. Immunity *38*, 1142–1153.
49. Liu, Q., Zhang, D., Hu, D., Zhou, X., and Zhou, Y. (2018). The role of mitochondria in NLRP3 inflammasome activation. Mol. Immunol. *103*, 115–124.
50. Mishra, S.R., Mahapatra, K.K., Behera, B.P., Patra, S., Bhol, C.S., Panigrahi, D.P., Praharaj, P.P., Singh, A., Patil, S., Dhiman, R., and Bhutia, S.K. (2021). Mitochondrial dysfunction as a driver of NLRP3 inflammasome activation and its modulation through mitophagy for potential therapeutics. Int. J. Biochem. Cell Biol. *136*, 106013.
51. Billingham, L.K., Stoolman, J.S., Vasan, K., Rodriguez, A.E., Poor, T.A., Szibor, M., Jacobs, H.T., Reczek, C.R., Rashidi, A., Zhang, P., et al. (2022). Mitochondrial electron transport chain is necessary for NLRP3 inflammasome activation. Nat. Immunol. *23*, 692–704.
52. Yabal, M., Calleja, D.J., Simpson, D.S., and Lawlor, K.E. (2019). Stressing out the mitochondria: Mechanistic insights into NLRP3 inflammasome activation. J. Leukoc. Biol. *105*, 377–399.
53. Zhou, R., Yazdi, A.S., Menu, P., and Tschopp, J. (2011). A role for mitochondria in NLRP3 inflammasome activation. Nature *469*, 221–225.
54. Meuren, L.M., Prestes, E.B., Papa, M.P., de Carvalho, L.R.P., Mustafá, Y.M., da Costa, L.S., Da Poian, A.T., Bozza, M.T., and Arruda, L.B. (2022). Infection of endothelial cells by dengue virus induces ROS production by different sources affecting virus replication, cellular activation, death and vascular permeability. Front. Immunol. *13*, 810376.
55. Heid, M.E., Keyel, P.A., Kamga, C., Shiva, S., Watkins, S.C., and Salter, R.D. (2013). Mitochondrial reactive oxygen species induces NLRP3-dependent lysosomal damage and inflammasome activation. J. Immunol. *191*, 5230–5238.
56. Sorbara, M.T., and Girardin, S.E. (2011). Mitochondrial ROS fuel the inflammasome. Cell Res. *21*, 558–560.
57. Harijith, A., Ebenezer, D.L., and Natarajan, V. (2014). Reactive oxygen species at the crossroads of inflammasome and inflammation. Front. Physiol. *5*, 352.
58. Minutoli, L., Puzzolo, D., Rinaldi, M., Irrera, N., Marini, H., Arcoraci, V., Bitto, A., Crea, G., Pisani, A., Squadrito, F., et al. (2016). ROS-Mediated NLRP3 Inflammasome Activation in Brain, Heart, Kidney, and Testis Ischemia/Reperfusion Injury. Oxid. Med. Cell. Longev. *2016*, 2183026.
59. Heinz, S., Freyberger, A., Lawrenz, B., Schladt, L., Schmuck, G., and Ellinger-Ziegelbauer, H. (2017). Mechanistic Investigations of the Mitochondrial Complex I Inhibitor Rotenone in the Context of Pharmacological and Safety Evaluation. Sci. Rep. *7*, 45465.
60. Liang, H.L., Sedlic, F., Bosnjak, Z., and Nilakantan, V. (2010). SOD1 and MitoTEMPO partially prevent mitochondrial permeability transition pore opening, necrosis, and mitochondrial apoptosis after ATP depletion recovery. Free Radic. Biol. Med. *49*, 1550–1560.
61. Hottz, E.D., Lopes, J.F., Freitas, C., Valls-de-Souza, R., Oliveira, M.F., Bozza, M.T., Da Poian, A.T., Weyrich, A.S., Zimmerman, G.A., Bozza, F.A., and Bozza, P.T. (2013). Platelets mediate increased endothelium permeability in dengue through NLRP3-inflammasome activation. Blood *122*, 3405–3414.
62. Pingen, M., Schmid, M.A., Harris, E., and McKimmie, C.S. (2017). Mosquito Biting Modulates Skin Response to Virus Infection. Trends Parasitol. *33*, 645–657.
63. Wang, J.P., Liu, P., Latz, E., Golenbock, D.T., Finberg, R.W., and Libraty, D.H. (2006). Flavivirus activation of plasmacytoid dendritic cells delineates key elements of TLR7 signaling beyond endosomal recognition. J. Immunol. *177*, 7114–7121.
64. Nasirudeen, A.M., Wong, H.H., Thien, P., Xu, S., Lam, K.P., and Liu, D.X. (2011). RIG-I, MDA5 and TLR3 synergistically play an important role in restriction of dengue virus infection. PLoS Neglected Trop. Dis. *5*, e926.
65. Uno, N., and Ross, T.M. (2018). Dengue virus and the host innate immune response. Emerg. Microb. Infect. *7*, 167.
66. Schneider, W.M., Chevillotte, M.D., and Rice, C.M. (2014). Interferon-stimulated genes: a complex web of host defenses. Annu. Rev. Immunol. *32*, 513–545.
67. Loo, Y.M., and Gale, M., Jr. (2011). Immune signaling by RIG-I-like receptors. Immunity *34*, 680–692.
68. Rodrigues de Sousa, J., Azevedo, R., Quaresma, J.A.S., and Vasconcelos, P. (2021). The innate immune response in Zika virus infection. Rev. Med. Virol. *31*, e2166.
69. Choudhury, S.M., Ma, X., Abdullah, S.W., and Zheng, H. (2021). Activation and Inhibition of the NLRP3 Inflammasome by RNA Viruses. J. Inflamm. Res. *14*, 1145–1163.
70. Zhao, C., and Zhao, W. (2020). NLRP3 Inflammasome-A Key Player in Antiviral Responses. Front. Immunol. *11*, 211.
71. Lupfer, C., and Kanneganti, T.D. (2013). The expanding role of NLRs in antiviral immunity. Immunol. Rev. *255*, 13–24.
72. Lai, J.H., Wang, M.Y., Huang, C.Y., Wu, C.H., Hung, L.F., Yang, C.Y., Ke, P.Y., Luo, S.F., Liu, S.J., and Ho, L.J. (2018). Infection with the dengue RNA virus activates TLR9 signaling in human dendritic cells. EMBO Rep. *19*.
73. Pan, Y., Cai, W., Cheng, A., Wang, M., Yin, Z., and Jia, R. (2022). Flaviviruses: Innate Immunity, Inflammasome Activation,

Inflammatory Cell Death, and Cytokines. Front. Immunol. *13*, 829433.
74. He, Z., An, S., Chen, J., Zhang, S., Tan, C., Yu, J., Ye, H., Wu, Y., Yuan, J., Wu, J., et al. (2020). Neural progenitor cell pyroptosis contributes to Zika virus-induced brain atrophy and represents a therapeutic target. Proc. Natl. Acad. Sci. USA *117*, 23869–23878.
75. Carod-Artal, F.J. (2018). Neurological complications of Zika virus infection. Expert Rev. Anti-Infect. Ther. *16*, 399–410.
76. Li, C., Xu, D., Ye, Q., Hong, S., Jiang, Y., Liu, X., Zhang, N., Shi, L., Qin, C.F., and Xu, Z. (2016). Zika Virus Disrupts Neural Progenitor Development and Leads to Microcephaly in Mice. Cell Stem Cell *19*, 120–126.
77. McCracken, M.K., Gromowski, G.D., Garver, L.S., Goupil, B.A., Walker, K.D., Friberg, H., Currier, J.R., Rutvisuttinunt, W., Hinton, K.L., Christofferson, R.C., et al. (2020). Route of inoculation and mosquito vector exposure modulate dengue virus replication kinetics and immune responses in rhesus macaques. PLoS Neglected Trop. Dis. *14*, e0008191.
78. Dudley, D.M., Newman, C.M., Lalli, J., Stewart, L.M., Koenig, M.R., Weiler, A.M., Semler, M.R., Barry, G.L., Zarbock, K.R., Mohns, M.S., et al. (2017). Infection via mosquito bite alters Zika virus tissue tropism and replication kinetics in rhesus macaques. Nat. Commun. *8*, 2096.
79. Sun, P., Nie, K., Zhu, Y., Liu, Y., Wu, P., Liu, Z., Du, S., Fan, H., Chen, C.H., Zhang, R., et al. (2020). A mosquito salivary protein promotes flavivirus transmission by activation of autophagy. Nat. Commun. *11*, 260.
80. Sadler, A.J., and Williams, B.R. (2008). Interferon-inducible antiviral effectors. Nat. Rev. Immunol. *8*, 559–568.
81. Ashley, C.L., Abendroth, A., McSharry, B.P., and Slobedman, B. (2019). Interferon-Independent Upregulation of Interferon-Stimulated Genes during Human Cytomegalovirus Infection is Dependent on IRF3 Expression. Viruses *11*.
82. Liang, Z., Wu, S., Li, Y., He, L., Wu, M., Jiang, L., Feng, L., Zhang, P., and Huang, X. (2011). Activation of Toll-like receptor 3 impairs the dengue virus serotype 2 replication through induction of IFN-β in cultured hepatoma cells. PLoS One *6*, e23346.
83. Hoang, L.T., Lynn, D.J., Henn, M., Birren, B.W., Lennon, N.J., Le, P.T., Duong, K.T., Nguyen, T.T., Mai, L.N., Farrar, J.J., et al. (2010). The early whole-blood transcriptional signature of dengue virus and features associated with progression to dengue shock syndrome in Vietnamese children and young adults. J. Virol. *84*, 12982–12994.
84. Sung, P.S., Huang, T.F., and Hsieh, S.L. (2019). Extracellular vesicles from CLEC2-activated platelets enhance dengue virus-induced lethality via CLEC5A/TLR2. Nat. Commun. *10*, 2402.
85. Coldbeck-Shackley, R.C., Eyre, N.S., and Beard, M.R. (2020). The Molecular Interactions Of ZIKV And DENV With The Type-I IFN Response. Vaccines *8*.
86. Gentry, M.K., Henchal, E.A., McCown, J.M., Brandt, W.E., and Dalrymple, J.M. (1982). Identification of distinct antigenic determinants on dengue-2 virus using monoclonal antibodies. Am. J. Trop. Med. Hyg. *31*, 548–555.
87. Calvet, G., Aguiar, R.S., Melo, A.S.O., Sampaio, S.A., de Filippis, I., Fabri, A., Araujo, E.S.M., de Sequeira, P.C., de Mendonça, M.C.L., de Oliveira, L., et al. (2016). Detection and sequencing of Zika virus from amniotic fluid of fetuses with microcephaly in Brazil: a case study. Lancet Infect. Dis. *16*, 653–660.

STAR★METHODS

KEY RESOURCES TABLE

REAGENT or RESOURCE	SOURCE	IDENTIFIER
Antibodies		
Stat-1(D1K9Y) Rabbit mAb	Cell Signaling	Cat#14994S RRID:AB_2737027
Phosho-Stat-1(Ser727)	Cell Signaling	Cat# 9177S RRID:AB_2197983
Caspase-1	Cell Signaling	Cat#2225 RRID:AB_2243894
IRF-3 (D6I4C) XP® Rabbit mAb	Cell Signaling	Cat# 11904 RRID:AB_2722521
Phospho-IRF-3(Ser396) (4D4G) Rabbit mAb	Cell Signaling	Cat# 4947 RRID:AB_823547
NF-κB p65 (D14E12) XP® Rabbit mAb	Cell Signaling	Cat# 8242 RRID:AB_10859369
Phospho-NF-κB p65 (Ser536) (93H1)	Cell Signaling	Cat# 3033 RRID:AB_331284
NF-κB1 p105/p50 (D4P4D) Rabbit mAb	Cell Signaling	Cat# 13586 RRID:AB_2665516
Syk (4D10) Mouse mAb	Cell Signaling	Cat# 80460 RRID:AB_2799953
Phospho-Syk (Tyr525/526) (C87C1) Rabbit mAb	Cell Signaling	Cat# 2710 RRID:AB_2197222
NLRP3 (D2P5E) Rabbit	Cell Signaling	Cat# 13158 RRID:AB_2798134
Human IL-1 beta/IL-1F2 Antibody	R&D Systems	Cat# AF-201-NA RRID:AB_354387
GAPDH	GeneTex	Cat# GTX100118
anti- goat IgG HRP conjugated	R&D Systems	Cat# HAF017 RRID:AB_562588
anti- sheep IgG HRP conjugated	R&D Systems	Cat# HAF016 RRID:AB_562591
Goat anti- rabbit IgG (H + L) HRP	invitrogen	Cat# 65-6120
Mouse IgG antibody 4G2	Gentry et al. (1982)[86] Provided by Dr. Steve Whitehead, NIAID, NIH.	N/A
Peroxidase-labeled goat anti-mouse IgG (used for virus titration)	SeraCare	Cat# 5450-0011; RRID: AB_2687537
Bacterial and virus strains		
2015 Fortaleza Zika virus strain	Calvet et al. (2016).[87] Provided by Dr. Steve Whitehead, NIAID, NIH.	N/A
DENV type 2 strain (DENV-2/US/BID-V594/2006)	BEI Resources	N/A
Chemicals, peptides, and recombinant proteins		
Rotenone	Milipore Sigma	Cat# CAS 83-79-4
Mito-Tempo	Enzo Life Sciences	Cat# ALX-430-150-M005
Blasticidin	Invivigon	Cat# anti-bl

(*Continued on next page*)

Continued

REAGENT or RESOURCE	SOURCE	IDENTIFIER
MCC 950	Adipogen	Cat# CAS 256373-96-3
Protease/phosphatase Inhibitor	Cell Signaling	Cat# 5872S
Phosphate buffer saline (PBS)	R&D Systems	Cat# DY006
Wash Buffer	R&D Systems	Cat# WA126
Reagent Diluent	R&D Systems	Cat# DY995
Substrate Solution	R&D Systems	Cat# DY999
Stop Solution	R&D Systems	Cat# DY994
SYTOX™ Green Nucleic Acid Stain	Thermo Fisher Scientific	Cat# S7020
Paraformaldehyde	Fisher Scientific	Cat# 50-980-487
Bovine Serum Albumin	Sigma-Aldrich	Cat# A9576
Triton X-100	EMD Millipore, Fisher Scientific	Cat# M1122980101
Dimethyl sulfoxide (DMSO)	Fisher Scientific	Cat# BP231-100
Sodium pyruvate	Gibco Thermo Fisher Scientific	Cat# 12539059
L-glutamine	Gibco, Thermo Fisher Scientific	Cat# 25030149
Non-essential amino acids	Gibco, Thermo Fisher Scientific	Cat# 11-140-050
Methylcellulose	Sigma-Aldrich	Cat# M0512
OptiMEM medium	Gibco Thermo Fisher Scientific	Cat# 31985062
Penicillin–Streptomycin–Amphotericin B	Gibco, Thermo Fisher Scientific	Cat# 15240096
Antibiotic-Antimycotic	Gibco, Thermo Fisher Scientific	Cat# 15240096
Zeocin	Invivogen	Cat# ant-zn-05
Normocin	Invivogen	Cat# ant-nr-1
Blasticidin	Invivogen	Cat# ant-bl-05
TrueBlue™ Peroxidase Substrate	Seracare	Cat# 5510-0030
RPMI 1640 media	Sigma-Aldrich	Cat# R8758
DMEM	Gibco Thermo Fisher Scientific	Cat# 11965092
Dermal Cell Basal Medium	ATCC	Cat# PCS-200-030
Keratinocyte Growth Kit	ATCC	Cat# PCS-200-040
Trypsin-EDTA for Primary Cells	ATCC	Cat# PCS-999-003
Fetal Bovine Serum	Gibco Thermo Fisher Scientific	Cat# 16000044
Phorbol-12-myristate-13-acetate (PMA)	Invivogen	Cat# tlrl-pma
Nigericin	Invivogen	Cat# tlrl-nig
ATP	Invivogen	Cat# tlrl-atpl
70-kDa FITC-dextran	Sigma-Aldrich	Cat# FD70S
Methanol	Fisher Scientific	Cat# A4524
Isopropanol	Fisher Scientific	Cat# 67-63-0
Chloroform	Fisher Scientific	Cat# C298-500
TrueBlue™ Peroxidase Substrate	SeraCare	Cat# 50-78-02
RIPA Lysis and Extraction Buffer	Thermo Fisher Scientific	Cat# 89900
Restore™ PLUS Western Blot Stripping Buffer	Thermo Fisher Scientific	Cat# 46430
DC™ Protein Assay Kit I	BIO-RAD	Cat# 5000112
NuPAGE™ 4 to 12%, Bis-Tris, 1.0–1.5 mm, Mini Protein Gels	Thermo Fisher Scientific	Cat# NP0321BOX
NuPAGE™ LDS Sample Buffer (4X)	Thermo Fisher Scientific	Cat# NP0007
TBS, Tris-Buffered Saline	Fisher Scientific	Cat# BP2471500

(*Continued on next page*)

Continued

REAGENT or RESOURCE	SOURCE	IDENTIFIER
Tween 20™	Fisher Scientific	Cat# AAJ20605AP
iBlot 2 PVDF Mini Stacks	Invitrogen Thermo Fisher Scientific	Cat# IB24002
SuperSignal™ West Femto Maximum Sensitivity Substrate	Thermo Fisher Scientific	Cat# 34096
Critical commercial assays		
DCFDA/H2DCFDA - Cellular ROS Assay Kit	Abcam	Cat# ab113851
Human IL-1 beta/IL-1F2 DuoSet ELISA	R&D Systems	Cat# DY201
Human Total IL-18 DuoSet ELISA	R&D Systems	Cat# DY318-05
Mouse IL-1 beta/IL-1F2 Quantikine ELISA Kit	R&D Systems	Cat# MLB00C
Human IL-8/CXCL8 DuoSet ELISA	R&D Systems	Cat# DY208
Human IL-6 DuoSet ELISA	R&D Systems	Cat# DY206
DCFDA/H2DCFDA - Cellular ROS Assay Kit	Abcam	Cat#ab113851
Caspase-Glo 1 Inflammasome Assay	Promega	Cat# G9951
Microvascular Endothelial Cell Growth Kit-BBE	ATCC	Cat# PCS-100-040
LunaScript® RT SuperMix Kit	New England Biolabs	Cat# E3010L
Luna® Universal qPCR Master Mix	New England Biolabs	Cat# M3003X
Experimental models: Cell lines		
C6/36 cells	ATCC	Cat# CRL-1660
THP-1 cells	ATCC	Cat# TIB-202
THP-1-KO-NLRP3	Invivogen	Cat# thp-konlrp3z
ASC expressing RAW 264.7 Cells	Invivogen	Cat# raw-asc
Vero cells	ATCC	Cat# CCL-81
Primary Epidermal Keratinocytes; Normal, Human, Neonatal Foreskin (HEKn)	ATCC	Cat# PCS-200-010
Experimental models: Organisms/strains		
Aedes aegypti Liverpool strain wild type	Virginia Tech, VA, USA	N/A
Oligonucleotides		
Primers for RelA, SYK, STAT-1, IRF-3, IRF-7, NF-kB, TLR-3, NLRP3, AIM2, Caspase-1, CXCL-10, CXCL-11, DDX58, IFB-beta, MX-1, OAS-2, DENV-1 NS5, ZIKV NS5, GAPDH see Table S1	This paper	N/A
Software and algorithms		
Gen 5 software	Biotek Instruments	https://www.biotek.com/products/software-robotics-software/gen5-microplate-reader-and-imager-software/
GraphPad Prism v 7	GraphPad Software	https://www.graphpad.com/
BioRender software	BioRender	https://biorender.com/
ImageJ software version 1.52a	Schneider et al., 2012	https://ImageJ.nih.gov/ij/
Azure 300 imaging system	Azure Biosystems	https://azurebiosystems.com/
ds-11 spectrophotometer	DeNovix	https://www.denovix.com/products/ds-11-fx-spectrophotometer-fluorometer/
CFX96 thermocycler	Biorad	https://www.bio-rad.com/

RESOURCE AVAILABILITY

Lead contact

Further information and requests for resources and reagents should be directed to and will be fulfilled by the lead contact, Eric Calvo (ecalvo@niaid.nih.gov).

Materials availability

All unique/stable reagents generated in this study are available from the lead contact with a completed materials transfer agreement.

Data and code availability

(1) No new custom code was generated for this paper.
(2) Any additional information required to reanalyze the data reported in this paper is available from the lead contact upon request.

EXPERIMENTAL MODEL AND SUBJECT DETAILS

All cell lines described were cultured under temperature-controlled conditions at 37°C and 5% CO2 with humidity. The cell lines have not been authenticated.

METHOD DETAILS

Cells and viruses

Human monocyte cells THP-1 (Cat. ATCC- TIB-202) were purchased from ATCC. Cells were grown in RPMI 1640, 2 mM L-glutamine, 25 mM HEPES, 10% (v/v) heat-inactivated fetal bovine serum (FBS), 100 U/mL penicillin, 100 μg/mL streptomycin, at 37°C following the manufacturer's instructions. THP-1-KO-NLRP3 human monocyte cells (Invivogen, CA, USA) were grown in RPMI 1640, 2 mM L-glutamine, 25 mM HEPES, 10% (v/v) heat-inactivated FBS, 100 U/ml penicillin, 100 μg/mL streptomycin, 100 μg/mL Normocin, 100 μg/mL Zeocin at 37°C following the manufacturer's instructions. THP-1 cells were differentiated into macrophages by plating the cells with 50 ng/mL PMA for 24 h followed by replacing with fresh culture media, and cells were allowed to differentiate for the next 48 h. ASC-expressing RAW 264.7 cells (murine macrophages) (Invivogen, CA, USA) were grown in DMEM, 4.5 g/L glucose, 4 mM L-glutamine, 10% heat-inactivated FBS, 100 U/ml penicillin, 100 μg/mL streptomycin, 100 μg/mL Normocin, 10 μg/mL Blasticidin following manufacturer's protocol. DENV type 2 strain (DENV-2/US/BID-V594/2006) was obtained from BEI Resources. The ZIKV strain Paraíba (Brazil, 2015) was provided by Dr. Steve Whitehead (NIAID/NIH) and propagated in C3/36 cells. These cells were grown in minimum essential medium (pH 7.2) supplemented with 10% FBS, sodium pyruvate, L-glutamine, and nonessential amino acids (NEAA) (Gibco, USA) and incubated at 37°C. ZIKV stocks were prepared by infecting a monolayer of C6/36 cells with 80%–85% confluence for 24 to 48 h. The supernatant was collected, and the cells were cleared by centrifugation at 1000 *x g* for 10 min at 4°C and concentrated in 0.22-micron Amicon columns to 1/10 of the starting volume. The stocks were aliquoted and stored at −80°C until further use.

DENV and ZIKV quantification

Virus titers were determined by plaque assay. Vero cells (ATCC, VA, USA) were seeded at a density of 1×10^5 cells per well in standard 24 well plates. Serial dilutions of culture supernatant were added and incubated for 2 h at 37°C. The cell monolayers were then overlaid with 1 mL/well of Opti-MEM (Gibco, Grand Island, NY, USA) containing 1% methylcellulose, 2% Fetal Bovine Serum, 2 mM L-glutamine, and 1 X antibiotic-antimycotic solution (Gibco, Grand Island, NY, USA). Plates were incubated at 37°C and 5% CO_2 for 4–5 days. After the overlay medium was discarded, plates were washed with 1 X phosphate-buffered saline (1X PBS buffer) and fixed at room temperature for 30 min with 80% methanol and blocked with 5% PBS milk for 20 min. Plates were washed and then incubated with mouse IgG antibody 4G2 (pan-flavivirus antibody provided by Dr. Steve Whitehead, NIAID, NIH) at 1:2000 dilution for 1 h. The primary antibody was removed, and plates were washed twice. Subsequently, peroxidase-labeled goat anti-mouse IgG was added to the plates at a 1:2000 dilution and incubated for 1 h. Finally, plates were washed, and TrueBlue Peroxidase substrate (KPL) was added to reveal the plaques. One-way ANOVA tests was used to determine statistical significance using GraphPad Prism software version 9.0.

Western blot analysis

Whole cell extracts were isolated using Pierce RIPA Buffer (Thermo Scientific, USA) supplemented with protease and phosphatase cocktail inhibitor (Abcam, Cambridge, UK). The concentrations of the isolated proteins were determined using the DC Protein Assay Kit II (Biorad, CA, USA). Thirty micrograms of protein from whole cell lysates were separated on NuPAGE 4–12% Bis-Tris gels (Invitrogen, MA, USA). The supernatant was removed from cells following stimulation and concentrated by adding 1/4 V of chloroform and 1 V of methanol to the harvested supernatants centrifuged at 12000 rpm for 5 min. The upper methanol layer was aspirated, and 1 V of methanol was added again and centrifuged at 12000 rpm for 5 min. Supernatants were removed and discarded, and the remaining pellet was resuspended in 30 μL 1x LDS sample buffer SDS-PAGE and separated on NuPAGE 4–12% Bis-Tris gels. Proteins were transferred to a nitrocellulose membrane using an iBlot machine (Invitrogen, USA) and then blocked for 1 h at 37°C with blocking buffer [5% (w/v) powdered nonfat milk in tris-buffered saline (TBS)-tween (0.1%)] and subsequently incubated in primary antibodies anti-caspase-1, anti-NLRP3, anti-NF-kB, anti-P-NF-kB p65, anti-P-NF-kB p50, anti-IRF-3, anti-P-IRF-3, anti-STAT-1, anti-SYK (Cell signaling, MA, USA), anti-IL-1β, anti-P-STAT-1, anti-P-SYK (R&D Systems, MN, USA), or anti-GAPDH (GeneTex, CA,

USA), overnight at 4°C. The membranes were washed two times with TBS-tween (0.1%) for 5 min each, and the membrane was then incubated for 1 h with secondary antibody goat anti-rabbit (Invitrogen, MA, USA), rabbit anti-goat, or donkey anti-sheep (R&D Systems, MN, USA), diluted in blocking buffer at room temperature. Immunogenic bands were developed with Super Signal West Femto Maximum Sensitivity Substrate (Thermo Scientific, USA). Blots were imaged using an Azure 300 imaging system (Azure Biosystems, USA).

Caspase Glo 1 inflammasome assay

Caspase-1 activities in culture supernatants were measured using Caspase Glo1 inflammasome assay according to the manufacturer's instructions (Promega, WI, USA). THP-1 cells were differentiated using PMA (phorbol 12-myristate-13-acetate) for 24 h, fresh medium was added without PMA, and the cells were incubated for 48 h. The cells were treated with LPS for 15 h, ATP (5 mM) for 1 h, DENV, ZIKV, DENV with *Ae. aegypti* SGE, ZIKV with *Ae. aegypti* SGE, or alone with *Ae. aegypti* SGE for 36 h. Fifty microliter aliquots of each concentrated supernatant were transferred to wells of a Corning 96-Well, Cell Culture-Treated, white-flat-bottom microplate (Fisher Scientific, NH, USA); 50 μL of Caspase Glo1 reagent was added, followed by mixing on a plate shaker at 300 RPM for 30 s. After 1 h at room temperature, the luminescence in each well was measured using a Cytation 5 reader. Luminescence in culture medium without cells was subtracted from the luminescence measured in wells containing cells.

Enzyme-linked immunosorbent assay (ELISA)

Concentrations of human IL-1β in culture supernatant were measured using human IL-1β/IL-1F2, while human IL-6 and IL-8 were measured using DuoSet ELISA according to the manufacturer's instructions (R&D Systems, MN, USA) at a 450 nm optical density. To measure IL-1β, IL-6, and IL-8 concentrations in the supernatants of THP-1 cells, PMA -differentiated THP-1 cells were treated with LPS for 15 h, ATP for 1 h, DENV, ZIKV, DENV with *Ae. aegypti* SGE, ZIKV with *Ae. aegypti* SGE, or alone with *Ae. aegypti* SGE for 36 h. A 100 μL aliquot of each supernatant was used for ELISA. Concentrations of mature human IL-1β, IL-6, and IL-8 were calculated using a standard curve.

Cell death assay

For measurement of THP-1 cell death, 50,000 PMA-differentiated cells were treated with LPS for 15 h, ATP for 1 h, DENV, ZIKV, DENV with *Ae. aegypti* SGE, ZIKV with *Ae. aegypti* SGE, or alone with *Ae. aegypti* SGE for 36 h in flat bottom black 96 well black clear bottom plates (Thermofisher, MA, USA) in a medium containing SYTOX Green Nucleic Acid Stain (50 nM, S7020, Invitrogen, MA, USA) in 200 μL media per well. After the treatment, fluorescence was measured using Cytation 5 reader (Excitation: 480 nm, Emission: 530 nm).

Reactive oxygen species detection

Reactive oxygen species (ROS) were measured using the cell permeant reagent 2′,7′-dichlorofluorescin diacetate (DCFDA) according to the manufacturer's protocol (Cat: ab113851, Abcam, Cambridge, UK) and measured using Cytation 5 reader (Excitation 488 nm, Emission: 530 nm).

Mosquito rearing, salivary gland dissection, and saliva collection

Aedes aegypti (Liverpool strain, LVP) mosquitoes were reared in standard insectary conditions (27°C, 80% humidity with a 12 h light/dark cycle) at the Laboratory of Malaria and Vector Research, NIAID, NIH. Salivary glands from sugar-fed adult mosquitoes (5–7 days old) were dissected in PBS, pH 7.4 under a stereomicroscope. *Aedes. aegypti* SGE was obtained by disrupting the gland walls by sonication (Fisher Brand, model FB120). Sonication was carried out at power 30% duty cycle (36W/20 kHz), with 3 cycles of 2 s pulse and 1 s rest (for 40 s) to allow dissipation of heat. A typical salivary gland homogenate (2–5 days old, sugar fed) yields approximately 2 μg of total protein. Tubes were centrifuged at 12,000 × *g* for 5 min, and supernatants were kept at −80°C until used.

Gene expression analysis

Differentiated THP-1 cells treated with DENV, ZIKV, DENV with *Ae. aegypti* SGE, ZIKV with *Ae. aegypti* SGE, or alone with *Ae. aegypti* SGE for 24 h were collected in Trizol (Thermofisher, MA, USA) and stored at −80°C. Total RNA was extracted with Trizol, according to the manufacturer's instructions. cDNA was prepared using the LunaScript RT SuperMix Kit (New England Biolabs, MA, USA) from 1 μg of extracted RNA. All experiments were carried out in technical replicates. All nucleic acid concentrations and OD 260/280 ratios were measured by a DS-11 spectrophotometer (DeNovix, USA). For qPCR, specific primers were designed and used (Table S1). Briefly, in a final volume of 20 μL, the reaction mixture was prepared with Luna Universal qPCR Master Mix (New England Biolabs, MA, USA), 300 nM of each forward and reverse primer, and 10 ng of cDNA template. Reactions were run on a CFX96 thermocycler (BioRad, USA) using the following amplification protocol: 95°C, 2 min; 40 cycles of 95°C,15 s; 60°C, 30 s. A melting curve (60°C–95°C) was initially included to evaluate primer specificity. All samples were analyzed in technical triplicates, and non-template controls were included as negative controls. qPCR data were manually examined and analyzed using the ΔΔCt method. ΔCt values were obtained by normalizing the data against the GAPDH housekeeping gene primer (Table S1). Untreated cell samples were used as ΔΔCt controls. The relative abundance of genes of interest, or fold change, with respect to the untreated cells was calculated as 2^ΔΔCt. Graphs were prepared using GraphPad Prism software version 9.0.

Statistical analysis

Results are expressed as mean ± SEM. Statistical differences among treatment groups were analyzed by *t*-test or one-way ANOVA using Tukey or Dunnett as a test for multiple comparisons. Significance was set at $p \leq 0.05$ (Graph-Pad Prism software, version 9.0).